



1 **From Canals to the Coast: Dissolved Organic Matter and Trace**
2 **Metal Composition in Rivers Draining Degraded Tropical**
3 **Peatlands in Indonesia**

4 Laure Gandois^a, Alison May Hoyt^{b*}, Stéphane Mounier^c, Gaël Le Roux^a, Charles Franklin
5 Harvey^{bd}, Adrien Claustres^a, Mohammed Nuriman^e, Gusti Anshari^e

6 ^a EcoLab, Université de Toulouse, CNRS, INPT, UPS, Toulouse, France

7 ^bDepartment of Civil & Environmental Engineering, Massachusetts Institute of Technology, Cambridge, MA
8 01239, USA

9 ^cPROTEE, Université de Toulon, F-83957, La Garde, France

10 ^d Center for Environmental Sensing and Modeling, Singapore-MIT Alliance for Research and Technology,
11 Singapore

12 ^eMagister of Environmental Science, and Soil Science Department, Universitas Tanjungpura (UNTAN),
13 Pontianak, West Kalimantan Province, Indonesia

14 *Present address: Max Planck Institute for Biogeochemistry, 07745 Jena, Germany

15 Corresponding author : ahoyt@bgc-jena.mpg.de
16

17 **Abstract.** Worldwide, peatlands are important sources of dissolved organic matter (DOM) and trace metals (TM) to
18 surface waters and these fluxes may increase with peatland degradation. In Southeast Asia, tropical peatlands are being
19 rapidly deforested and drained. The black rivers draining these peatland areas have high concentrations of DOM, and
20 the potential to be hotspots for CO₂ release. However, the fate of this fluvial carbon export is uncertain, and its role as
21 a trace metal carrier has never been investigated. This work aims to address these gaps in our understanding of tropical
22 peatland DOM and associated elements in the context of degraded tropical peatlands of Indonesian Borneo. We
23 quantified dissolved organic carbon and trace metals concentrations in the dissolved and fine colloidal (<0.22µm) and
24 coarse colloidal (0.22 – 2.7 µm) fractions and characterized the characteristics (δ¹³C, Absorbance, Fluorescence
25 :excitation-emission matrix and PARAFAC analysis) of the peatland-derived DOM as it drains from peatland canals,
26 flows along the blackwater Ambawang River, and eventually mixes with Kapuas Kecil River before meeting the ocean
27 near the city of Pontianak in West Kalimantan, Indonesia. We observe downstream shifts in indicators of in-stream
28 processing. The increase in the δ¹³C of DOC, along with an increase in the C1/C2 ratio of PARAFAC fluorophores,
29 and decrease in SUVA (Specific UV Absorbance) along the continuum suggest the predominance of photo-oxidation.
30 However, we also observe very low dissolved oxygen concentrations, suggesting that oxygen is quickly consumed by
31 microbial degradation of DOM in the shallow layers of water. Black rivers draining degraded peatlands show
32 significantly higher concentrations of Al, Fe, Pb, As, Ni, and Cd. A strong association is observed between DOM, Fe,
33 As, Cd and Zn in the dissolved and fine colloid fraction, while Al is associated to Pb and Ni and present in a higher



34 proportion in the coarse colloidal fraction. We additionally measure the isotopic composition of lead released from
35 degraded tropical peatlands for the first time and show that Pb originates from anthropogenic atmospheric deposition.
36 Degraded tropical peatlands are important sources of DOM and trace metals to rivers and a secondary source of
37 atmospherically deposited contaminants.

38 **Keywords:** Tropical peatlands, Dissolved Organic Matter, Absorbance, Fluorescence, PARAFAC, Stable isotopes,
39 Trace metal, Lead isotopes

40 1. Introduction

41 Most Southeast Asian tropical peatlands developed as domes beneath ombrotrophic peat swamp forests (Page et al.,
42 2006; Cobb et al. 2017). They store at least 68.5 Pg C, or 15-19% of the global peat carbon stocks (Page et al., 2011;
43 Dargie et al., 2017; Läfteenoja et al., 2012). They have experienced widespread degradation as a result of deforestation,
44 conversion to agriculture and drainage, which all accelerated in the late 1970s (Miettinen et al., 2011). This abrupt
45 change in land use, and corresponding lowering of the water table, has led to subsidence and a massive release of
46 carbon from peatlands to the atmosphere due to enhanced aerobic decomposition of organic matter from the drained
47 peat. Extensive work has focused on quantifying the resulting CO₂ fluxes (Couwenberg et al., 2010; Jauhiainen et al.,
48 2012; Miettinen et al., 2017) and land surface subsidence (e.g. (Hooijer et al., 2012; Carlson et al., 2015).

49 Drainage canals are dug in forested peatlands for multiple reasons: first, as a mechanism to transport timber out of the
50 peatland during deforestation, and later to lower the water table, making the land suitable for agriculture. These
51 peatland drainage canals channel water from the peatlands to surrounding surface waters. The resulting fluvial export
52 of dissolved organic matter (DOM) has been recognized as a significant component of the carbon budget of tropical
53 peatlands, that could increase with deforestation and peatland exploitation (Gandois et al., 2013; Moore et al., 2011).
54 Indonesia alone contributes over 10% of the global riverine dissolved organic carbon (DOC) input into the ocean
55 (Baum et al., 2007), as a result of both high peatland coverage and high precipitation rates. This proportion is likely to
56 increase with rapid peatland conversion to agriculture, which destabilizes long-term peat C stocks (Moore et al., 2013).

57 Another implication of DOM transfers from peatlands to surface water is the transport of associated elements,
58 especially trace metals (TM). Tropical peatlands in Southeast Asia are mainly ombrotrophic systems, which receive
59 critical nutrients through atmospheric deposition, and serve as a sink for atmospheric pollutants (Weiss et al., 2002).
60 Northern peatlands have been shown to constitute a source of major and trace elements to surface waters (Broder and
61 Biester, 2017; Jeremiason et al., 2018; Rothwell et al., 2007). This has important implication : as a result of colloidal
62 association between peatland-derived organic molecules and Fe, northern peatlands are responsible for a significant
63 transfer of Fe to the Atlantic Ocean (Krachler et al. 2010, 2012). In the UK, peat degradation and erosion has led to
64 the dispersion of lead into watersheds, which previously accumulated through atmospheric deposition over decades
65 (Rothwell et al., 2008). Although drainage of tropical peatlands is occurring at a rapid rate across Southeast Asia, to
66 our knowledge no data are available on trace metal release in black rivers draining tropical peatlands.



67 Black rivers draining peatlands (as defined in (Alkhatib et al., 2007)) also have the potential to be hotspots of fluvial
68 carbon degassing (Müller et al., 2015; Wit et al., 2015). By measuring pCO₂ in Indonesian and Malaysian black rivers,
69 Wit et al. (2015) estimated that 53% of DOC entering surface waters was converted to CO₂, which is similar to global
70 averages for inland waters. In contrast, blackwater river measurements and incubations by Martin et al., (2018) found
71 a smaller proportion of DOC was processed in rivers. Rixen et al., (2008) also found a large proportion of the DOM
72 was resistant to decomposition in a laboratory incubation study. These studies have focused on CO₂ measurements and
73 incubations to assess the potential for DOM processing.

74 Monitoring changes in DOM composition in canals and rivers can provide complementary information on the extent
75 of in-stream processing of fluvial carbon, and potential reemission of greenhouse gas (GHG) to the atmosphere.
76 Qualitative evaluation of in-stream DOM transformation by UV light and microbial processes can be performed using
77 isotopic and optical characterization of DOM. The stable isotope signature of DOM is an indicator of its origin (Barber
78 et al., 2017; Hood et al., 2005), but also transformation processes. Lalonde et al (2014) assessed photochemical
79 processing of DOM in major large rivers worldwide, and found that it caused an increase in the δ¹³C of DOM of 0.5
80 to 2.3%. However, microbial processing is also expected to lead to an increase in the δ¹³C of DOM. Optical properties
81 of DOM are also sensitive indicators for DOM processing (Hansen et al., 2016; Harun et al., 2015; Spencer et al.,
82 2009), with contrasted effects on optical properties. Microbial processing is generally found to increase the aromaticity
83 of DOM by selective processing of less aromatic molecules, while photo-oxidation tends to decrease aromaticity,
84 because of selective photo-oxidation of aromatic moieties (Spencer et al., 2009; Hansen et al., 2016).

85 In summary, although there has been an increase in efforts to quantify DOC exports from tropical peatlands, our
86 complementary understanding of the transfer of associated elements and in-stream processing of DOM remains limited.
87 This work aims to address these gaps in our understanding of the composition and evolution of tropical peatland DOM
88 and how it could act as a carrier of trace metals to surface waters, in the context of highly degraded tropical peatlands
89 of Indonesia. We characterize the quality of the peatland-derived DOM and trace metals as they drain from peatland
90 canals, flow along blackwater rivers, and eventually mix with a whitewater river before meeting the ocean. We assess
91 spatial and seasonal changes in the organic matter quality, and document changes in DOM composition due to
92 transport, mixing, and processing. We also assess black river trace metal release to surface waters, analyzing trace
93 metal concentrations and the isotopic composition of lead released from degraded tropical peatlands for the first time.

94 **2. Material and methods**

95 **2.1 Study area**

96 The study area is located in West Kalimantan, Indonesia, near the city of Pontianak (0.09°N, 109.24°E) on the island
97 of Borneo. The climate is humid equatorial with 2953±564 mm of rainfall and a mean annual temperature of 27°C
98 (1985-2017 data). The monthly annual rainfall ranges from 170±126 mm (August) to 349±98 mm (November). The
99 highest rainfalls are measured from October to January. The mean rainfall is 274 ± 123 mm for January, and 199 ±
100 106 mm for June. (Figure SI.1). The study focused on the Ambawang River, which flows into the Landak and Kapuas



101 Kecil rivers. It is a black river draining a watershed (approximately 706 km²) entirely covered with peatlands. This
102 river was selected to represent water of exclusively peatland origin. All peatlands in the sampling area have been
103 drained and converted to agriculture.

104 2.2 Sample collection and treatment

105 Two sampling campaigns were conducted in June 2013 (drier period) and January 2014 (wetter period). Using a boat,
106 samples were collected in the center of the river, from the origin of the Ambawang river (BR, black river sites) to its
107 downstream confluence with the Landak and Kapuas Kecil Kecil (WR, white river sites). White river samples collected
108 upstream of the confluence with the white river (WRu). Drainage canals (DC) flowing into the black river were also
109 sampled during the second sampling campaign. In January 2014, a rain collector was installed on the roof of the
110 Pontianak's meteorological station to collect rain samples for lead isotopic analysis. In situ parameters (pH,
111 conductivity and dissolved oxygen) were measured using a multiparameter probe (WTW, Germany). Depth profiles
112 of dissolved oxygen in the black river were also measured with an oxygen microelectrode (MI-730 dip-type micro-
113 oxygen electrode and O2-ADPT adapter; Microelectrodes, Inc., Bedford, NH, USA). Frequent calibration was
114 performed with a zero oxygen solution and distilled water equilibrated to ambient oxygen concentrations, where
115 temperature was carefully monitored. To create the zero oxygen solution, 1 g of sodium sulfite (Na₂S₀₃) and a few
116 crystals (~1 mg) of cobalt chloride (CoCl₂) was dissolved in 1 L of distilled water. For measurements of additional
117 parameters, a larger volume of water was collected for further analysis. Samples were filtered immediately following
118 collection on the boat using a portable peristaltic pump (Geotech, USA) and prebaked and pre-weighed GF/F filters
119 (0.7 μm) and stored in glass bottles for DOC, δ¹³C-DOC and optical properties of DOM analysis. Samples were filtered
120 with cellulose acetate filters (0.22 μm) and stored in polypropylene vials for analysis of major nutrients and trace
121 element. DOC analysis was repeated on the cellulose acetate samples and DOC concentrations did not differ
122 significantly based on filtration at 0.2 or 0.7 μm. In January 2014, at selected sites (8), samples were first filtered with
123 GF/D filters (2.7 μm) to assess to the coarse colloidal fraction of trace metals and DOC.

124 3. Sample analysis

125 Non-purgeable organic carbon (NPOC, referred to hereafter as DOC) was analyzed on filtered (GF/F Whatman)
126 samples after acidification to pH 2 (HCl) with a TOC-V CSH analyzer (Shimadzu, Japan), with a quantification limit
127 of 1 mg L⁻¹. Major cations and anions were analysed using an HPLC (Dionex, USA). The quantification limit was 0.5
128 mg L⁻¹ for chloride, nitrate and sulphates and 0.025 mg L⁻¹ for ammonium, potassium, magnesium and calcium.
129 Certified material (ion 915 and ion 96.4 Environment and Climate Change Canada, Canada) was included in the
130 analytical loop and recovery was >95% of the certified value. For trace element analysis, samples were acidified with
131 ultrapure HNO₃ prior to ICP-MS (7500 ce, Agilent Technologies) analysis. ¹¹⁵In was used as an internal standard, and
132 SLRS-4 (River water certified for trace elements) was used as a reference material on every run and accuracy
133 (recovery>95%) was checked. Determination limits were < 0.5 μg g⁻¹ for Fe and Al, <0.05 μg g⁻¹ for Ni, Cu and Zn
134 and < 0.005 μg g⁻¹ for Cd and Pb. Pb isotope ratios (²⁰⁶Pb/²⁰⁷Pb; ²⁰⁸Pb/²⁰⁶Pb) in water samples were analyzed using a



135 High Resolution ICP-MS (Thermo Element II XR; OMP service ICP-MS, Toulouse, France). Measurements were
136 corrected for mass bias using individual sample bracketing with certified and adequately diluted NIST NBS-981 (100
137 ng L^{-1} to 500 ng L^{-1}) according to Krachler et al. (2004).

138 The UV absorption spectra of pore water were measured with a spectrophotometer (Secoman UVi-lightXT5) from 190
139 to 700 nm in a 1 cm quartz cell. The Specific UV Absorbance at 254 nm (SUVA, $\text{L mg}^{-1} \text{ m}^{-1}$) was calculated as follows:
140 $\text{SUVA} = A_{254}/(b \cdot \text{DOC})$ (Weishaar et al., 2003), where A_{254} is the sample absorbance at 254 nm (non-dimensional), b
141 is the optical path length (m) and DOC is in mg L^{-1} . The baseline was determined with ultra-pure water.

142 Emission Excitation Matrices (EEM) were acquired using a Hitachi F4500 fluorescence spectrometer. Emission
143 spectra were acquired from 250 to 550 nm for excitation ranging from 250 to 550 nm. The slits were set to 5 nm for
144 both the excitation and emission monochromators. The scan speed was 2400 nm min^{-1} and the integration response
145 was 0.1 s. Fluorescence intensity was corrected from the excitation beam to ensure stability. The inner filter effect
146 water was taken into account using a dilution approach as developed by Luciani et al. (2009). The fluorescence index
147 was calculated as defined by McKnight et al. (2001) and Jaffé et al. (2008), by the ratio of the fluorescence intensity
148 at 470 nm to the fluorescence intensity at 520 nm for a 370 nm excitation. The PARAFAC analysis (PARAllel FACTor
149 analysis (Bro, 1997)) was performed on all samples using the PROGMEEF program in Matlab (Luciani et al., 2008).

150 The isotopic composition ($\delta^{13}\text{C}$) of DOC was determined at the UC Davis Stable Isotope Facility, following the
151 described procedure (<http://stableisotopefacility.ucdavis.edu/doc.html>). Briefly, a TOC Analyzer (OI Analytical,
152 College Station, TX) is interfaced to a PDZ Europa 20-20 isotope ratio mass spectrometer (Sercon Ltd., Cheshire, UK)
153 utilizing a GD-100 Gas Trap Interface (Graden Instruments).

154 **4. Statistical analysis**

155 Statistical analysis was performed using the Rstudio software (Version 1.2.1335), using ggplot, dplyr, ade4 and
156 dunn.test packages. Significant differences ($p < 0.05$) between groups were evaluated using Kruskal Wallis and Dunn's
157 post hoc multiple test.

158 **5. Results**

159 **5.1. Trends in water chemistry from the source of the black river to the ocean**

160 The observed water chemistry of the Ambawang river and drainage canals is typical of black rivers draining peatlands
161 (Table 1, Figure 2), and does not show significant differences between the two sampling seasons. It is acidic with a pH
162 of 3.2 ± 0.6 and 3.5 ± 0.3 in the drainage canals (DC) and black river (BR) respectively, has a low conductivity (DC:
163 $89.8 \pm 21.4 \mu\text{S cm}^{-1}$, BR: $85.2 \pm 21.6 \mu\text{S cm}^{-1}$), is anoxic (DC: 2.3 ± 0.3 , BR: $1.9 \pm 0.7 \text{ mg L}^{-1}$), and has extremely high
164 DOC concentrations (DC: 35.2 ± 5.5 , BR: $35.8 \pm 3.4 \text{ mg L}^{-1}$). The Cl concentrations are low and homogeneous (DC:
165 2.6 ± 0.7 , BR: $2.4 \pm 0.6 \text{ mg L}^{-1}$). After the confluence with the White River, the chemistry of the river radically changes.



166 An abrupt increase in pH is observed (WR: 5.3 ± 0.7). The dissolved oxygen concentration increases up to 3.7 ± 1.0 mg
167 L⁻¹ and DOC concentrations drop sharply to 9.2 ± 3.2 mg L⁻¹. Across all samples, the DOC concentrations show a
168 significant negative correlation with DO concentrations ($r^2=0.63$, $n=40$, $p<4.10^9$). In contrast, no increase in Cl is
169 observed until close to the ocean (3 samples corresponding to ocean water intrusion were excluded from Figure 2).
170 After the confluence with the black river, The DOC/Cl ratio also drops sharply from 15 in the black river and drainage
171 canals to 5 in the white river (Figure SI.2).

172 5.2. DOM optical characteristics and stable isotopic signature

173 No systematic differences were observed for the DOM characteristics between the two sampling campaigns. The $\delta^{13}\text{C}$
174 signature of DOC (Figure 3a) is very negative, reaching $-30.3 \pm 0.4\text{‰}$ in the drainage canals. It increases along the
175 continuum from upstream in the black river to the ocean. Significant differences are observed between the drainage
176 canals and black river compared to the white river. The $\delta^{13}\text{C}$ signature of DOC is significantly negatively correlated
177 with DOC concentration ($r^2=0.68$, $p<10^{-4}$, $n=40$), with the highest DOC values being associated with the lowest $\delta^{13}\text{C}$ -
178 DOC values.

179 The SUVA index (Figure 3b) shows high values in the black river (5.3 ± 1.2), the highest values measured upstream. A
180 wide range of values is measured in the drainage canals (4.3 ± 1.4). The SUVA values of the Black River are
181 significantly higher than those measured in the Kapuas Kecil (4.5 ± 0.3) and its tributaries (4.2 ± 0.2). The fluorescence
182 index varies widely in the drainage canals (1.60 ± 0.17) and black river (1.55 ± 0.06), but is more uniform in the white
183 river, both upstream (1.55 ± 0.03) and downstream (1.55 ± 0.05) of the confluence with the Black river. These two optical
184 indices show coherent spatial patterns within the black river and drainage canals (Figure 3b&d), with lower SUVA
185 values being associated with higher FI values, in 3 drainage canals and in the black river close to their connection,
186 sampled during the second sampling campaign. Across all samples, a significant correlation is observed between FI
187 and SUVA values ($r^2=0.37$, $p<10^{-4}$, $n=41$).

188 The EEMS of all water samples have two main peaks (Figure SI.3). The main one ($\lambda_{\text{ex}}=250$ nm, $\lambda_{\text{em}}=460$ nm), is
189 coupled with a less intense peak ($\lambda_{\text{ex}}=350$ nm, $\lambda_{\text{em}}=460$ nm). The peaks are typical of high molecular and aromatic
190 molecules, which have been observed in wetlands (Fellman et al., 2010). The PARAFAC analysis reveals two
191 fluorophores: C1 ($\lambda_{\text{ex}}=255$ nm, $\lambda_{\text{em}}=450$ nm) and C2 ($\lambda_{\text{ex}}=285$ nm, $\lambda_{\text{em}}=485$ nm, Figure SI. 3) The first component
192 constitutes from 60 to 73 % of the total fluorescence of samples. The relative contribution of these two fluorophores
193 evolves along the sampled continuum, with the lowest values measured upstream in the black river (Figure 3c). The
194 spatial evolution of C1/C2 ratio and $\delta^{13}\text{C}$ -DOC are consistent. A significant ($r^2=0.43$, $p<0.001$, $n=41$) relationship is
195 observed across all the samples. A stronger relationship ($r^2=0.85$, $p<0.001$, $n=5$) is observed when the drainage canals
196 samples alone are considered.

197 5.3. Trace element concentrations and physical fractionation



198 Black rivers originating from drained peatlands have a unique composition of inorganic elements. The concentrations
199 of trace metals (Pb, Ni, Zn, Cd) as well as Al and Fe and are significantly higher in the black river and drainage canals
200 than the concentrations in the white river (Table 1, Figure 4). For Al, Fe and As, high concentrations were measured
201 in the Black River during the first sampling campaign (drier conditions). In contrast to other TM, higher Cu
202 concentrations are measured in the white river. A PCA analysis (Figure 5) of TM concentration and DOM properties
203 reveals specific association between DOC, Fe and As and to a lesser extend Zn and Cd, while another group is formed
204 by Al, Pb and Ni (Figure 5). Cu shows no association with DOM but does show increased concentrations with higher
205 FI. The first axis of PCA (load of DOC, Fe, As) strongly discriminates the black river and drainage canals samples
206 from the white river.

207 The distribution of DOC and TM is presented in Table 2. Dissolved organic matter is mostly (>98%) in the dissolved
208 and fine colloids form (<0,22 μm) all along the studied continuum. Iron and As are mostly present in the form of
209 dissolved and fine colloids in the black river and drainage canals (>96%). However, after transfer to the white river,
210 half of Fe and a third of As is in the coarse colloidal form. Zinc and Cd do not show similar patterns. Aluminium is
211 mostly present in the coarse colloidal phase (>60%) in the black river and drainage canal and this proportion further
212 increases in the white river (>80%). Lead is mostly present in the dissolved and fine colloid phase (>75%) in the
213 drainage canals and black river and shifts to coarse colloidal (>60%) forms after the confluence with the white river.
214 Nickel and Cu is mostly present in the dissolved and fine colloidal phase in the DC and BR but almost entirely in the
215 coarse colloidal fraction in the white river.

216 **5.4. Pb isotopic composition**

217 We observe distinct differences between the lead isotope ratios in the white river and those in the black river and
218 drainage canals. A decrease in the $^{206}\text{Pb}/^{207}\text{Pb}$ isotopic ratio is observed with increasing Pb concentrations in the black
219 river but not the white river (Figure 6a). Furthermore, the biplot of the $^{206}\text{Pb}/^{207}\text{Pb}$ and the $^{208}\text{Pb}/^{206}\text{Pb}$ signatures
220 illustrates significant differences between the white water and black river/drainage canal groups (Figure 6b).

221 **6. Discussion**

222 **6.1. In-stream processing of DOM in black rivers**

223 We observe in-stream processing of DOM, but the total DOM exported from tropical peatlands exceeds the processing
224 capacity of the rivers which drain them and a large proportion of DOM is transported to the ocean. We find persistently
225 high DOC concentrations in both drainage canals and black rivers draining degraded peatlands consistent with the
226 range of previously reported values in Borneo (Moore et al., 2013; Cook et al., 2018) and in the upper range of black
227 rivers in Sumatra (Rixen et al., 2008; Baum et al., 2007). We also find indicators of in-stream processing of DOM.
228 The transformation of DOM we observe along the continuum is likely due to dominant photo-oxidation and a lower
229 contribution of microbial processing. We observe an increase in the $\delta^{13}\text{C}$ -DOC values along the studied continuum
230 (Figure 3a). This shift toward higher $\delta^{13}\text{C}$ -DOC is correlated with an increase in the C1/C2 ratio of PARAFAC



231 fluorophores (Figure 3c). The two fluorophores are typical of terrestrial input of DOM (Yamashita et al., 2008). An
232 increase in this C1/C2 ratio reflects a shift toward lower wavelengths and therefore toward lower aromaticity and lower
233 molecular weight (Austnes et al., 2010). Moreover, a decreasing trend of SUVA values is observed along the
234 continuum (Figure 3b). These observations indicate that at our site, aromatic features are preferentially processed in-
235 stream, consistent with a dominant effect of photo-oxidation (Amon and Benner, 1996; Sharpless et al., 2014; Spencer
236 et al., 2009). This has also been observed in the Congo River where photo-oxidation led to an increase in $\delta^{13}\text{C}$ -DOC
237 and a decrease in aromatic features (Spencer et al., 2009).

238 However, photo-oxidation is not the only process responsible of DOM processing. The low oxygen levels in the black
239 river and drainage canals and the significant relationship between DOC and DO concentrations suggest that nearly all
240 oxygen entering the well-mixed water is quickly consumed by DOM oxidation (Figure 2a&b). The sharply decreasing
241 oxygen profiles measured in the black river suggest that the transformation of DOM is restricted to the shallow surface
242 layers of these waters (Figure SI.4). Additionally, localized increases in fluorescence index (reflecting a higher
243 proportion of microbial derived DOM, Figure 3d) suggest that extensive microbial processing occurs in some, but not
244 all locations in drainage canals and before it is transferred to the black river. Both photo-oxidation and microbial
245 processing have been quantified in laboratory experiments for DOM originating from tropical peatlands. Martin et al.
246 (2018) found that up to 25 % of riverine DOC from a black river in Sarawak, Malaysia, was lost within 5 days of
247 exposure to natural sunlight. Microbial long-term incubation studies by Rixen et al. (2008), showed that 27% of DOC
248 was degraded after two weeks, and that as a whole, 73 % of DOC was considered refractory to microbial degradation.
249 Another hypotheses is that in-stream microbial processing of DOM is further limited by the low pH, and low nutrient
250 levels (especially inorganic nitrogen), of the Black River (Wickland et al., 2018), rather than intrinsic refractory
251 characteristics. Although the precise extent of in-stream processing cannot be quantified here, our results are consistent
252 with in stream transformation of DOM by important photo-oxidation but also microbial degradation in the shallow
253 surface layers. Additionally, quantitative assessment of outgassing in tropical peatland drainage canals would improve
254 the evaluation of carbon release following peatland drainage. Overall, more work is needed to understand the extent
255 of upstream processing of peatland DOM.

256 **6.2. Role of DOM, Al and Fe in trace metal dynamics in peat draining waters**

257 This study provides the first record of trace metals in black rivers originating from degraded tropical peatlands. We
258 observe strong enrichment of Al and Fe, as well as Pb, As, Ni and Cd in peat-draining waters. The measured
259 concentrations are comparable to those measured by Kurasaki et al. (2000) in Borneo rivers for Pb, Zn, Cu and Cd, but
260 significantly higher (5 to 10 times) for Fe. The concentration levels, however, remain low compared to highly impacted
261 regions of Indonesia (Arifin et al., 2012). The elevated concentrations of Al and Fe in water draining tropical peatlands
262 is consistent with existing observations of elevated Fe concentrations from black rivers in the tropics (Zhang et al.,
263 2019) and northern peatlands. This enrichment is likely due to the weathering of mineral material under the peat during
264 peat accumulation processes (Tipping et al., 2002; Pokrovsky et al., 2005). As a consequence, in water draining
265 peatlands, strong organo-mineral associations between DOM and Fe (Krachler et al. 2010, 2012; Broder and Biester



266 2015), as well as DOM and Al (Helmer et al., 1990) have been observed. These colloidal associations between DOM
267 and Al and Fe in the form of hydroxides strongly control TM transfer and speciation in peat draining waters (Tipping
268 et al., 2002). In the present study, specific associations of trace metals with Al and Fe are observed, including strong
269 links between Al and Pb and Ni. However, the lack of a direct relationship between Pb and DOM contrasts with
270 reported observations in the literature (Graham et al., 2006; Jeremiason et al., 2018; Pokrovsky et al., 2016). Despite
271 this, we do observe strong links between Fe, As, Zn, Cd and DOM, which have been previously reported in water
272 draining peatlands (Broder and Biester, 2015; Neubauer et al., 2013; Pokrovsky et al., 2016). The coupled dynamic
273 of Fe and As might be related to similar mobilization processes within the peat column, with the sorption of As to
274 Fe(III)-(oxyhydr)oxides (ThomasArrigo et al., 2014) in anoxic peat water. Widespread drainage of tropical peatlands
275 and the corresponding release of anoxic water to surface water networks could induce a coupled increase in DOM and
276 Fe concentrations, similar to that which has occurred in Sweden (Kritzberg and Ekström, 2011).

277 **6.3. Peatlands as secondary sources of atmospheric pollutants**

278 The isotopic composition of Pb in peat draining water strongly suggests its anthropogenic origin. The isotopic
279 signatures measured in river samples are a combination of the signature of undisturbed soils of Borneo (Valentine et
280 al., 2008), and a mix of both present and past anthropogenic inputs. Older anthropogenic inputs are reflected by the
281 signature of atmospheric deposition from Java aerosols (Bollhöfer and Rosman, 2000), while the signature of recent
282 regional anthropogenic inputs was characterized by rain samples collected in Pontianak as part of this study (Figure
283 6b). In the black river and drainage canals, the isotopic ratio is close to the aerosols and recently sampled rainwater
284 and dominated by anthropogenic inputs, whereas the isotopic ratio in the white river is closer to the natural signal
285 (Figure 6). This isotopic difference is consistent with the difference between the watersheds drained by these two
286 rivers: tropical peatlands are ombrotrophic systems, and the trace metal content in peat soil is derived from the
287 atmosphere (Weiss et al., 2002), whereas the Kapus Kecil is recharged from a larger watershed and reflects contribution
288 of mineral soils. Tropical peatlands can serve as secondary sources of atmospheric pollutants to the environment. With
289 peatland drainage, black rivers release the accumulated atmospheric deposition over hundreds of years on much shorter
290 timescales. For example, the isotopic signature observed in the black river reflects anthropogenic sources deposited at
291 different times, including older deposition such as the lead measured in the Java aerosols (Bollhöfer and Rosman,
292 2000), and more recent deposition following the widespread introduction of unleaded fuel (characterized by samples
293 collected from rainwater during the January 2014 sampling period in this study). This release of lead by degraded
294 tropical peatlands has the potential to impact records from environmental archives, for example the [corals](#) of the
295 Singapore Strait (Chen et al., 2015). Although this is the first measurement of the aquatic release of trace metals from
296 tropical peatlands, the role of tropical peatlands as a secondary source of contaminants has also been highlighted by
297 the trace metal content analysis of dust emitted to the atmosphere by peat fires (Betha et al., 2013).

298 **6.4. From degraded tropical peatlands to the ocean**

299 Sharp changes in physico-chemical conditions are observed after the mixing of the black and the white river, including
300 sharp increases in DO concentration and pH values. This strongly controls the transport of DOM and TM drained from



301 degraded tropical peatlands. After the confluence with the white river, DOC concentrations decrease abruptly. At the
302 same time, the DOC/Cl ratio decreases sharply from the black river and drainage canals to the white river. This suggests
303 that dilution alone is insufficient to explain the drop in DOC concentrations. Instead, in stream processing of DOM
304 likely plays a role, with the sudden elevation of pH and DO creating favorable conditions for microbial processing of
305 DOC, making the mixing zone a likely hotspot of GHG emissions (Palmer et al., 2016). This would also be consistent
306 with the decrease in the SUVA index observed after the confluence. Despite processing of DOM in the mixing zone,
307 a significant proportion of DOM originating from degraded peatlands actually reaches ocean. We observe high DOC
308 concentrations at all sampling locations, with concentrations remaining high even close to the ocean (Figure 2a).
309 Additionally, the results of our physical fractionation show that even close to the estuary, DOC remains in the dissolved
310 and fine colloid form ($<0.22 \mu\text{m}$), and that flocculation processes might be limited. The decrease in trace metal
311 concentrations after the confluence might be influenced by shifts in physical fractionation and increase proportion of
312 colloidal form. This is especially true for Al and Pb. Some flocculation at the estuary might limit their transfer to the
313 ocean. A higher proportion of Fe and As remains in the form of fine colloids after mixing with the whiter river, and is
314 still associated with DOC. Similar conservative behavior of LMW organic molecules associated with Fe was observed
315 at the outlet of northern peatlands (Krachler et al., 2012), and in Arctic rivers (Pokrovsky et al., 2014). This highlights
316 that dissolved organic molecules derived from tropical peatlands can also act as carriers of trace metals to the ocean.

317 7. Conclusions

318 This study characterizes the composition and concentration of DOM and TM in the canals and rivers draining the
319 degraded tropical peatlands of Indonesian Borneo. It highlights in-stream processing of DOM in drainage canals and
320 rivers draining degraded peatlands. Both stable isotopic and optical properties of DOM are consistent with photo-
321 oxidation along the continuum from the black river to the ocean. In the black river and drainage canals, rates of
322 microbial processing are likely limited by the low dissolved oxygen concentrations, and concentrated at shallow depths.
323 In contrast, after mixing with the white river, higher rates of microbial processing of DOM are expected. Along the
324 continuum, DOM is found at relatively high concentrations in the dissolved and fine colloidal phases, suggesting a
325 substantial fraction of DOM derived from degraded peatlands reaches the ocean. Additionally, we provide the first
326 assessment of trace metal concentrations in rivers draining degraded tropical peatlands. Rivers draining these peatlands
327 are enriched in some trace metals (Pb, Ni, Zn, Cd) as well as Al and Fe. Using the isotopic signature of Pb, we show
328 that degraded tropical peatlands are secondary sources of atmospherically deposited contaminants to surface waters.
329 Trace metal dynamics after transfer to the white river show clear trends: while Pb and Ni are associated with Al, As,
330 Zn and Cd are associated with Fe and DOM. Lead and Al are present in coarse colloidal form and may be transferred
331 to sediments after flocculation. In contrast, DOM, Fe and As are found predominantly in fine colloidal form even after
332 the confluence with the white river, and as a result may be transferred to the ocean. The role of degraded tropical
333 peatlands as a source of DOM, as well as Fe and As to the ocean requires further investigation.

334 Author contribution



335 LG, AMH, GH and CFH designed the study. LG, AMH, MN and GH conducted field campaigns. SM and LG
336 conducted fluorescence analysis. GLR and AC conducted lead isotope analysis. LG and AMH wrote the manuscript,
337 with inputs from all co-authors.

338 **Competing interests**

339 The authors declare no competing interests.

340 **Data availability**

341 The authors declare that the data supporting the findings are available within the article and from the authors upon
342 request.

343 **Acknowledgements**

344 This project was funded by the PEER project “Assessing Degradation of Tropical Peat Domes and Dissolved Organic
345 Carbon (DOC) Export from the Belait, Mempawah and Lower Kapuas Kecil Rivers in Borneo” lead by G. A. A.M.H.
346 and C.F.H were supported by the National Research Foundation Singapore through the Singapore–MIT Alliance for
347 Research and Technology’s Center for Environmental Sensing and Modeling Interdisciplinary Research Program, and
348 by the US National Science Foundation under Grants 1114155 and 1114161 (to C.F.H.). The authors thank F. Julien,
349 V. Payre-Suc and D. Lambrigt for DOC and major elements analysis (PAPC platform, EcoLab laboratory).

350 **References**

- 351 Alkhatib, M., Jennerjahn, T. C. and Samiaji, J.: Biogeochemistry of the Dumai River estuary, Sumatra, Indonesia, a
352 tropical black-water river, *Limnol. Oceanogr.*, 52(6), 2410–2417, doi:10.4319/lo.2007.52.6.2410, 2007.
- 353 Amon, R. M. W. and Benner, R.: Photochemical and microbial consumption of dissolved organic carbon and dissolved
354 oxygen in the Amazon River system, *Geochim. Cosmochim. Acta*, 60(10), 1783–1792, doi:10.1016/0016-
355 7037(96)00055-5, 1996.
- 356 Arifin, Z., Puspitasari, R. and Miyazaki, N.: Heavy metal contamination in Indonesian coastal marine ecosystems: A
357 historical perspective, *Coast. Mar. Sci.*, 35(1), 227–233, 2012.
- 358 Austnes, K., Evans, C. D., Eliot-Laize, C., Naden, P. S. and Old, G. H.: Effects of storm events on mobilisation and
359 in-stream processing of dissolved organic matter (DOM) in a Welsh peatland catchment, *Biogeochemistry*, 99(1), 157–
360 173, doi:10.1007/s10533-009-9399-4, 2010.
- 361 Barber, A., Sirois, M., Chaillou, G. and Gélinas, Y.: Stable isotope analysis of dissolved organic carbon in Canada’s
362 eastern coastal waters, *Limnol. Oceanogr.*, 62(S1), S71–S84, doi:10.1002/lno.10666, 2017.
- 363 Baum, A., Rixen, T. and Samiaji, J.: Relevance of peat draining rivers in central Sumatra for the riverine input of
364 dissolved organic carbon into the ocean, *Estuar. Coast. Shelf Sci.*, 73(3–4), 563–570, doi:10.1016/j.ecss.2007.02.012,
365 2007.
- 366 Betha, R., Pradani, M., Lestari, P., Joshi, U. M., Reid, J. S. and Balasubramanian, R.: Chemical speciation of trace
367 metals emitted from Indonesian peat fires for health risk assessment, *Atmospheric Res.*, 122(Supplement C), 571–578,
368 doi:10.1016/j.atmosres.2012.05.024, 2013.



- 369 Bollhöfer, A. and Rosman, K. J. R.: Isotopic source signatures for atmospheric lead: the Southern Hemisphere,
370 *Geochim. Cosmochim. Acta*, 64(19), 3251–3262, doi:10.1016/S0016-7037(00)00436-1, 2000.
- 371 Bro, R.: PARAFAC. Tutorial and applications - ScienceDirect, *Chemom. Intell. Lab. Syst.*, 149–171, 1997.
- 372 Broder, T. and Biester, H.: Hydrologic controls on DOC, As and Pb export from a polluted peatland – the importance
373 of heavy rain events, antecedent moisture conditions and hydrological connectivity, *Biogeosciences*, 12(15), 4651–
374 4664, doi:https://doi.org/10.5194/bg-12-4651-2015, 2015.
- 375 Broder, T. and Biester, H.: Linking major and trace element concentrations in a headwater stream to DOC release and
376 hydrologic conditions in a bog and peaty riparian zone, *Appl. Geochem.*, 87, 188–201,
377 doi:10.1016/j.apgeochem.2017.11.003, 2017.
- 378 Carlson, K. M., Goodman, L. K. and May-Tobin, C. C.: Modeling relationships between water table depth and peat
379 soil carbon loss in Southeast Asian plantations, *Environ. Res. Lett.*, 10(7), 074006, doi:10.1088/1748-
380 9326/10/7/074006, 2015.
- 381 Chen, M., Lee, J.-M., Nurhati, I. S., Switzer, A. D. and Boyle, E. A.: Isotopic record of lead in Singapore Straits during
382 the last 50 years: Spatial and temporal variations, *Mar. Chem.*, 168, 49–59, doi:10.1016/j.marchem.2014.10.007, 2015.
- 383 Cobb, A. R., Hoyt, A. M., Gandois, L., Eri, J., Dommain, R., Salim, K. A., Kai, F. M., Su`ut, N. S. H. and Harvey, C.
384 F.: How temporal patterns in rainfall determine the geomorphology and carbon fluxes of tropical peatlands, *Proc. Natl.
385 Acad. Sci.*, 114(26), E5187–E5196, doi:10.1073/pnas.1701090114, 2017.
- 386 Cook, S., Whelan, M. J., Evans, C. D., Gauci, V., Peacock, M., Garnett, M. H., Kho, L. K., Teh, Y. A. and Page, S.
387 E.: Fluvial organic carbon fluxes from oil palm plantations on tropical peatland, *Biogeosciences*, 15(24), 7435–7450,
388 doi:https://doi.org/10.5194/bg-15-7435-2018, 2018.
- 389 Couwenberg, J., Dommain, R. and Joosten, H.: Greenhouse gas fluxes from tropical peatlands in south-east Asia, *Glob.
390 Change Biol.*, 16(6), 1715–1732, doi:10.1111/j.1365-2486.2009.02016.x, 2010.
- 391 Dargie, G. C., Lewis, S. L., Lawson, I. T., Mitchard, E. T. A., Page, S. E., Bocko, Y. E. and Ifo, S. A.: Age, extent and
392 carbon storage of the central Congo Basin peatland complex, *Nature*, 542(7639), 86–90, doi:10.1038/nature21048,
393 2017.
- 394 Fellman, J. B., Hood, E. and Spencer, R. G. M.: Fluorescence spectroscopy opens new windows into dissolved organic
395 matter dynamics in freshwater ecosystems: A review, *Limnol. Oceanogr.*, 55(6), 2452–2462,
396 doi:10.4319/lo.2010.55.6.2452, 2010.
- 397 Gandois, L., Cobb, A. R., Hei, I. C., Lim, L. B. L., Salim, K. A. and Harvey, C. F.: Impact of deforestation on solid
398 and dissolved organic matter characteristics of tropical peat forests: implications for carbon release, *Biogeochemistry*,
399 114(1), 183–199, doi:10.1007/s10533-012-9799-8, 2013.
- 400 Graham, M. C., Vinogradoff, S. I., Chipchase, A. J., Dunn, S. M., Bacon, J. R. and Farmer, J. G.: Using Size
401 Fractionation and Pb Isotopes to Study Pb Transport in the Waters of an Organic-Rich Upland Catchment, *Environ.
402 Sci. Technol.*, 40(4), 1250–1256, doi:10.1021/es0517670, 2006.
- 403 Hansen, A. M., Kraus, T. E. C., Pellerin, B. A., Fleck, J. A., Downing, B. D. and Bergamaschi, B. A.: Optical properties
404 of dissolved organic matter (DOM): Effects of biological and photolytic degradation, *Limnol. Oceanogr.*, 61(3), 1015–
405 1032, doi:10.1002/lno.10270, 2016.
- 406 Harun, S., Baker, A., Bradley, C., Pinay, G., Boomer, I. and Liz Hamilton, R.: Characterisation of dissolved organic
407 matter in the Lower Kinabatangan River, Sabah, Malaysia, *Hydrol. Res.*, 46(3), 411–428, doi:10.2166/nh.2014.196,
408 2015.



- 409 Helmer, E. H., Urban, N. R. and Eisenreich, S. J.: Aluminum geochemistry in peatland waters, *Biogeochemistry*, 9(3),
410 doi:10.1007/BF00000601, 1990.
- 411 Hood, E., Williams, M. W. and McKnight, D. M.: Sources of dissolved organic matter (DOM) in a Rocky Mountain
412 stream using chemical fractionation and stable isotopes, *Biogeochemistry*, 74(2), 231–255, doi:10.1007/s10533-004-
413 4322-5, 2005.
- 414 Hooijer, A., Page, S., Jauhiainen, J., Lee, W. A., Lu, X. X., Idris, A. and Anshari, G.: Subsidence and carbon loss in
415 drained tropical peatlands, *Biogeosciences*, 9(3), 1053–1071, doi:10.5194/bg-9-1053-2012, 2012.
- 416 Jaffé, R., McKnight, D., Maie, N., Cory, R., McDowell, W. H. and Campbell, J. L.: Spatial and temporal variations in
417 DOM composition in ecosystems: The importance of long-term monitoring of optical properties, *J. Geophys. Res.*
418 *Biogeosciences*, 113(G4), doi:10.1029/2008JG000683, 2008.
- 419 Jauhiainen, J., Hooijer, A. and Page, S. E.: Carbon Dioxide emissions from an Acacia plantation on peatland in
420 Sumatra, Indonesia, , doi:https://doi.org/10.5194/bg-9-617-2012, 2012.
- 421 Jeremiason, J. D., Baumann, E. I., Sebestyen, S. D., Agather, A. M., Seelen, E. A., Carlson-Stehlin, B. J., Funke, M.
422 M. and Cotner, J. B.: Contemporary Mobilization of Legacy Pb Stores by DOM in a Boreal Peatland, *Environ. Sci.*
423 *Technol.*, 52(6), 3375–3383, doi:10.1021/acs.est.7b06577, 2018.
- 424 Krachler, M., Roux, G. L., Kober, B. and Shotyk, W.: Optimising accuracy and precision of lead isotope measurement
425 (206 Pb, 207 Pb, 208 Pb) in acid digests of peat with ICP-SMS using individual mass discrimination correction, *J.*
426 *Anal. At. Spectrom.*, 19(3), 354–361, doi:10.1039/B314956K, 2004.
- 427 Krachler, R., Krachler, R. F., von der Kammer, F., Süphandag, A., Jirsa, F., Ayromlou, S., Hofmann, T. and Keppler,
428 B. K.: Relevance of peat-draining rivers for the riverine input of dissolved iron into the ocean, *Sci. Total Environ.*,
429 408(11), 2402–2408, doi:10.1016/j.scitotenv.2010.02.018, 2010.
- 430 Krachler, R., von der Kammer, F., Jirsa, F., Süphandag, A., Krachler, R. F., Plessl, C., Vogt, M., Keppler, B. K. and
431 Hofmann, T.: Nanoscale lignin particles as sources of dissolved iron to the ocean: NANOSCALE LIGNIN
432 PARTICLES, *Glob. Biogeochem. Cycles*, 26(3), n/a-n/a, doi:10.1029/2012GB004294, 2012.
- 433 Kritzberg, E. S. and Ekström, S. M.: Increasing iron concentrations in surface waters – a factor behind brownification?,
434 *Biogeosciences Discuss.*, 8(6), 12285–12316, doi:10.5194/bgd-8-12285-2011, 2011.
- 435 Kurasaki, M., Hartoto, D. I., Saito, T., Suzuki-Kurasaki, M. and Iwakuma, T.: Metals in Water in the Central
436 Kalimantan, Indonesia, *Bull. Environ. Contam. Toxicol.*, 65(5), 591–597, doi:10.1007/s0012800164, 2000.
- 437 Lähteenoja, O., Reátegui, Y. R., Räsänen, M., Torres, D. D. C., Oinonen, M. and Page, S.: The large Amazonian
438 peatland carbon sink in the subsiding Pastaza-Marañón foreland basin, Peru, *Glob. Change Biol.*, 18(1), 164–178,
439 doi:10.1111/j.1365-2486.2011.02504.x, 2012.
- 440 Lalonde, K., Vähätalo, A. and Gélinas, Y.: Revisiting the disappearance of terrestrial dissolved organic matter in the
441 ocean: a $\delta^{13}\text{C}$ study, *Biogeosciences*, 11(13) [online] Available from: <https://jyx.jyu.fi/handle/123456789/44281>
442 (Accessed 17 June 2019), 2014.
- 443 Luciani, X., Mounier, S., Paraquetti, H. H. M., Redon, R., Lucas, Y., Bois, A., Lacerda, L. D., Raynaud, M. and Ripert,
444 M.: Tracing of dissolved organic matter from the SEPETIBA Bay (Brazil) by PARAFAC analysis of total
445 luminescence matrices, *Mar. Environ. Res.*, 65(2), 148–157, doi:10.1016/j.marenvres.2007.09.004, 2008.
- 446 Luciani, X., Mounier, S., Redon, R. and Bois, A.: A simple correction method of inner filter effects affecting FEEM
447 and its application to the PARAFAC decomposition, *Chemom. Intell. Lab. Syst.*, 96(2), 227–238,
448 doi:10.1016/j.chemolab.2009.02.008, 2009.



- 449 Martin, P., Cherukuru, N., Tan, A. S. Y., Sanwlani, N., Mujahid, A. and Müller, M.: Distribution and cycling of
450 terrigenous dissolved organic carbon in peatland-draining rivers and coastal waters of Sarawak, Borneo, ,
451 doi:<http://dx.doi.org/10.5194/bg-15-6847-2018>, 2018.
- 452 McKnight, D. M., Boyer, E. W., Westerhoff, P. K., Doran, P. T., Kulbe, T. and Andersen, D. T.: Spectrofluorometric
453 characterization of dissolved organic matter for indication of precursor organic material and aromaticity, *Limnol.*
454 *Oceanogr.*, 46(1), 38–48, doi:10.4319/lo.2001.46.1.0038, 2001.
- 455 Miettinen, J., Shi, C. and Liew, S. C.: Deforestation rates in insular Southeast Asia between 2000 and 2010, *Glob.*
456 *Change Biol.*, 17(7), 2261–2270, doi:10.1111/j.1365-2486.2011.02398.x, 2011.
- 457 Miettinen, J., Hooijer, A., Vernimmen, R., Liew, S. C. and Page, S. E.: From carbon sink to carbon source: extensive
458 peat oxidation in insular Southeast Asia since 1990, *Environ. Res. Lett.*, 12(2), 024014, doi:10.1088/1748-
459 9326/aa5b6f, 2017.
- 460 Moore, S., Gauci, V., Evans, C. D. and Page, S. E.: Fluvial organic carbon losses from a Bornean blackwater river,
461 *Biogeosciences*, 8, 901–909, 2011.
- 462 Moore, S., Evans, C. D., Page, S. E., Garnett, M. H., Jones, T. G., Freeman, C., Hooijer, A., Wiltshire, A. J., Limin, S.
463 H. and Gauci, V.: Deep instability of deforested tropical peatlands revealed by fluvial organic carbon fluxes, *Nature*,
464 493(7434), 660–663, doi:10.1038/nature11818, 2013.
- 465 Müller, D., Warneke, T., Rixen, T., Müller, M., Jamahari, S., Denis, N., Mujahid, A. and Notholt, J.: Lateral carbon
466 fluxes and CO₂ outgassing from a tropical peat-draining river, *Biogeosciences Discuss.*, 12(13), 10389–10424,
467 doi:10.5194/bg-12-10389-2015, 2015.
- 468 Neubauer, E., von der Kammer, F., Knorr, K.-H., Peiffer, S., Reichert, M. and Hofmann, T.: Colloid-associated export
469 of arsenic in stream water during stormflow events, *Chem. Geol.*, 352, 81–91, doi:10.1016/j.chemgeo.2013.05.017,
470 2013.
- 471 Page, S. E., Rieley, J. O. and Wüst, R.: Chapter 7 Lowland tropical peatlands of Southeast Asia, in *Developments in*
472 *Earth Surface Processes*, vol. 9, edited by I. P. Martini, A. Martínez Cortizas, and W. Chesworth, pp. 145–172,
473 Elsevier., 2006.
- 474 Page, S. E., Rieley, J. O. and Banks, C. J.: Global and regional importance of the tropical peatland carbon pool, *Glob.*
475 *Change Biol.*, 17(2), 798–818, doi:10.1111/j.1365-2486.2010.02279.x, 2011.
- 476 Palmer, S. M., Evans, C. D., Chapman, P. J., Burden, A., Jones, T. G., Allott, T. E. H., Evans, M. G., Moody, C. S.,
477 Worrall, F. and Holden, J.: Sporadic hotspots for physico-chemical retention of aquatic organic carbon: from peatland
478 headwater source to sea, *Aquat. Sci.*, 78(3), 491–504, doi:10.1007/s00027-015-0448-x, 2016.
- 479 Pokrovsky, O. S., Dupré, B. and Schott, J.: Fe–Al–organic Colloids Control of Trace Elements in Peat Soil Solutions:
480 Results of Ultrafiltration and Dialysis, *Aquat. Geochem.*, 11(3), 241–278, doi:10.1007/s10498-004-4765-2, 2005.
- 481 Pokrovsky, O. S., Shirokova, L. S., Viers, J., Gordeev, V. V., Shevchenko, V. P., Chupakov, A. V., Vorobieva, T. Y.,
482 Candaudap, F., Causserand, C., Lanzanova, A. and Zouiten, C.: Fate of colloids during estuarine mixing in the Arctic,
483 *Ocean Sci.*, 10(1), 107–125, doi:10.5194/os-10-107-2014, 2014.
- 484 Pokrovsky, O. S., Manasypov, R. M., Loiko, S. V. and Shirokova, L. S.: Organic and organo-mineral colloids in
485 discontinuous permafrost zone, *Geochim. Cosmochim. Acta*, 188, 1–20, doi:10.1016/j.gca.2016.05.035, 2016.
- 486 Rixen, T., Baum, A., Pohlmann, T., Balzer, W., Samiaji, J. and Jose, C.: The Siak, a tropical black water river in central
487 Sumatra on the verge of anoxia, *Biogeochemistry*, 90(2), 129–140, doi:10.1007/s10533-008-9239-y, 2008.



- 488 Rothwell, J. J., Evans, M. G., Daniels, S. M. and Allott, T. E. H.: Baseflow and stormflow metal concentrations in
489 streams draining contaminated peat moorlands in the Peak District National Park (UK), *J. Hydrol.*, 341(1), 90–104,
490 doi:10.1016/j.jhydrol.2007.05.004, 2007.
- 491 Rothwell, J. J., Evans, M. G., Daniels, S. M. and Allott, T. E. H.: Peat soils as a source of lead contamination to upland
492 fluvial systems, *Environ. Pollut.*, 153(3), 582–589, doi:10.1016/j.envpol.2007.09.009, 2008.
- 493 Sharpless, C. M., Aeschbacher, M., Page, S. E., Wenk, J., Sander, M. and McNeill, K.: Photooxidation-Induced
494 Changes in Optical, Electrochemical, and Photochemical Properties of Humic Substances, *Environ. Sci. Technol.*,
495 48(5), 2688–2696, doi:10.1021/es403925g, 2014.
- 496 Spencer, R. G. M., Stubbins, A., Hernes, P. J., Baker, A., Mopper, K., Aufdenkampe, A. K., Dyda, R. Y., Mwamba,
497 V. L., Mangangu, A. M., Wabakanghanzi, J. N. and Six, J.: Photochemical degradation of dissolved organic matter
498 and dissolved lignin phenols from the Congo River, *J. Geophys. Res. Biogeosciences*, 114(G3),
499 doi:10.1029/2009JG000968, 2009.
- 500 ThomasArrigo, L. K., Mikutta, C., Byrne, J., Barmettler, K., Kappler, A. and Kretzschmar, R.: Iron and Arsenic
501 Speciation and Distribution in Organic Flocs from Streambeds of an Arsenic-Enriched Peatland, *Environ. Sci.*
502 *Technol.*, 48(22), 13218–13228, doi:10.1021/es503550g, 2014.
- 503 Tipping, E., Rey-Castro, C., Bryan, S. E. and Hamilton-Taylor, J.: Al(III) and Fe(III) binding by humic substances in
504 freshwaters, and implications for trace metal speciation, *Geochim. Cosmochim. Acta*, 66(18), 3211–3224,
505 doi:10.1016/S0016-7037(02)00930-4, 2002.
- 506 Valentine, B., Kamenov, G. D. and Krigbaum, J.: Reconstructing Neolithic groups in Sarawak, Malaysia through lead
507 and strontium isotope analysis, *J. Archaeol. Sci.*, 35(6), 1463–1473, doi:10.1016/j.jas.2007.10.016, 2008.
- 508 Weishaar, J. L., Aiken, G. R., Bergamaschi, B. A., Fram, M. S., Fujii, R. and Mopper, K.: Evaluation of Specific
509 Ultraviolet Absorbance as an Indicator of the Chemical Composition and Reactivity of Dissolved Organic Carbon,
510 *Environ. Sci. Technol.*, 37(20), 4702–4708, doi:10.1021/es030360x, 2003.
- 511 Weiss, D., Shotyk, W., Rieley, J., Page, S., Gloor, M., Reese, S. and Martinez-Cortizas, A.: The geochemistry of major
512 and selected trace elements in a forested peat bog, Kalimantan, SE Asia, and its implications for past atmospheric dust
513 deposition, *Geochim. Cosmochim. Acta*, 66(13), 2307–2323, doi:10.1016/S0016-7037(02)00834-7, 2002.
- 514 Wickland, K. P., Aiken, G. R., Butler, K., Dornblaser, M. M., Spencer, R. G. M. and Striegl, R. G.: Biodegradability
515 of dissolved organic carbon in the Yukon River and its tributaries: Seasonality and importance of inorganic nitrogen,
516 *Glob. Biogeochem. Cycles*, doi:10.1029/2012GB004342@10.1002/(ISSN)1944-9224.AQUNETWRK1, 2018.
- 517 Wit, F., Müller, D., Baum, A., Warneke, T., Pranowo, W. S., Müller, M. and Rixen, T.: The impact of disturbed
518 peatlands on river outgassing in Southeast Asia, *Nat. Commun.*, 6, 10155, doi:10.1038/ncomms10155, 2015.
- 519 Yamashita, Y., Jaffé, R., Maie, N. and Tanoue, E.: Assessing the dynamics of dissolved organic matter (DOM) in
520 coastal environments by excitation emission matrix fluorescence and parallel factor analysis (EEM-PARAFAC),
521 *Limnol. Oceanogr.*, 53(5), 1900–1908, doi:10.4319/lo.2008.53.5.1900, 2008.
- 522 Zhang, X., Müller, M., Jiang, S., Wu, Y., Zhu, X., Mujahid, A., Zhu, Z., Muhamad, M. F., Sia, E. S. A., Jang, F. H. A.
523 and Zhang, J.: Distribution and Flux of Dissolved Iron of the Rajang and Blackwater Rivers at Sarawak, Borneo,
524 *Biogeosciences Discuss.*, 1–31, doi:https://doi.org/10.5194/bg-2019-204, 2019.

525



526 **Table 1.** Water chemistry of the white river, black river and drainage canals for the two sampling campaigns (June: drier period, January, wetter period). The first line is the
 527 mean and the second line is the standard deviation. DO: Dissolved oxygen, FI: Fluorescence Index, SUVA: Specific UV Absorbance.

	pH	DO	Cond	DOC	$\delta^{13}\text{C}_{\text{DOC}}$	FI	SUVA	ClC2	Cl	Al	Fe	Pb	As	Zn	Cu	Ni	Cd	
Unit	/	mg L ⁻¹	$\mu\text{S cm}^{-1}$	mg L ⁻¹	%	-	L mg ⁻¹ m ⁻¹	mg L ⁻¹	mg L ⁻¹	$\mu\text{g L}^{-1}$	$\mu\text{g L}^{-1}$	$\mu\text{g L}^{-1}$	$\mu\text{g L}^{-1}$	$\mu\text{g L}^{-1}$	$\mu\text{g L}^{-1}$	$\mu\text{g L}^{-1}$	$\mu\text{g L}^{-1}$	
White River	June	5.20	4.49	37.2	8.43	-29.46	1.51	4.28	2.26	4.83	312.160	444.893	0.262	0.28	18.572	1.140	0.528	0.005
		0.33	0.26	13.2	1.61	0.23	0.03	0.00	0.08	4.03	407.057	383.954	0.236	0.09	9.028	0.158	0.106	0.002
	Jan.	4.43	3.37	1220.6	11.25	-29.41	1.60	4.57	2.30	409.16	147.242	547.500	0.129	0.32	10.264	0.868	1.186	0.006
		0.86	0.96	987.8	4.29	0.41	0.04	0.33	0.18	342.02	124.616	497.278	0.102	0.09	6.136	0.089	1.169	0.003
White River	June	5.45	4.91	24.0	6.89	-29.32	1.55	n.a	2.54	1.31	101.610	242.500	0.139	0.21	15.290	1.059	0.519	0.003
Upstream		5.71	0.17	3.8	1.28	0.06	0.08		0.22	0.64	27.490	44.500	0.027	0.02	3.060	0.007	0.077	0.000
	Jan.	5.37	4.15	268.7	8.69	-29.56	1.56	4.15	2.30	47.87	148.617	408.733	0.236	0.30	9.702	1.186	0.724	0.003
		0.06	0.39	92.0	0.78	0.13	0.01	0.15	0.14	65.16	71.999	170.153	0.167	0.04	6.233	0.244	0.441	0.000
Black River	June	3.45	1.69	98.7	36.42	-30.29	1.50	5.97	1.77	2.78	592.804	2143.500	0.467	0.59	119.386	0.582	1.958	0.012
		0.06	0.39	18.2	2.54	0.38	0.06	0.46	0.07	0.50	43.008	187.609	0.054	0.04	86.473	0.194	1.672	0.006
	Jan.	2.97	1.98	77.3	35.37	-30.04	1.59	4.94	2.12	2.19	443.136	1440.991	0.316	0.40	10.948	0.720	1.294	0.007
		0.13	0.75	18.3	3.70	0.38	0.15	1.32	0.15	0.57	137.488	493.547	0.110	0.10	6.980	1.127	0.527	0.003
Drainage canal	Jan.	3.08	2.34	89.8	35.17	-30.27	1.60	4.33	2.05	2.57	489.183	1348.017	0.313	0.35	14.518	0.369	1.535	0.008
		0.43	0.30	19.6	5.47	0.40	0.17	1.27	0.18	0.64	194.889	494.078	0.048	0.08	11.620	0.070	0.801	0.006

528

529

530

531

532

533



534

535 **Table 2.** Proportion of DOC and selected trace metals in the form of dissolved and fine colloids (< 0.22 µm) and coarse colloids (0.2-2.7 µm)

536

	Drainage Canals		Black River		White River	
	<0.2 µm	0.2-2.7 µm	<0.2 µm	0.2-2.7 µm	<0.2 µm	0.2-2.7 µm
DOC	97	3	98	2	100	0
Al	39	61	36	64	18	82
Fe	100	0	99	1	45	55
Pb	75	25	78	22	34	66
As	98	2	96	4	67	33
Ni	72	28	50	50	1	99
Cu	68	32	48	52	1	99
Zn	13	87	12	88	26	74
Cd	66	34	100	0	83	17

537

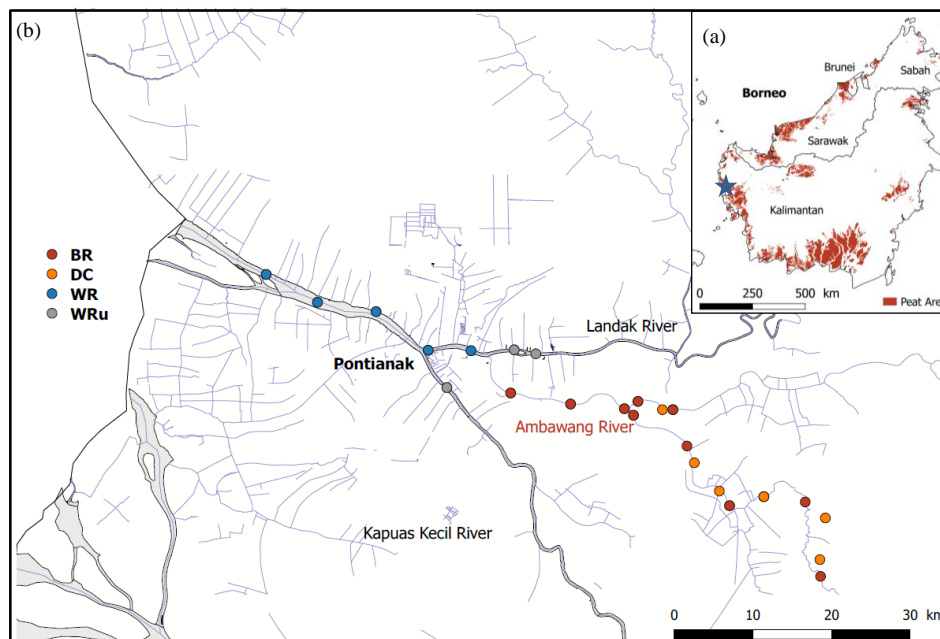


538

539

540

541



542

543 **Figure 1:** (a) Location of the study area on Borneo island. (b) Location of sampling sites and types of water: Black
544 River (BR), Drainage Canals (DC), White River (WR), and white River upstream of the confluence with the black
545 river (WRu).

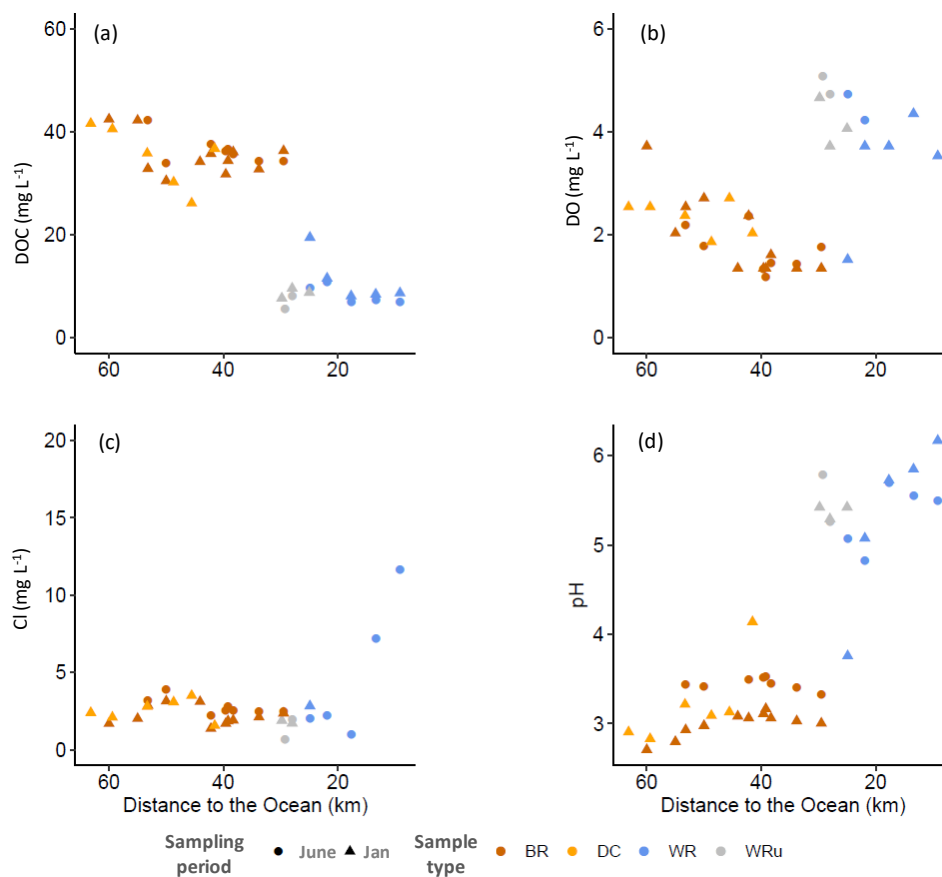
546

547

548



549
550
551
552
553
554
555



556

557 **Figure 2:** Evolution of (a) dissolved organic carbon concentration, (b) dissolved oxygen concentration, (c) chloride
558 concentration and (d) pH along the continuum from the black river to the ocean.

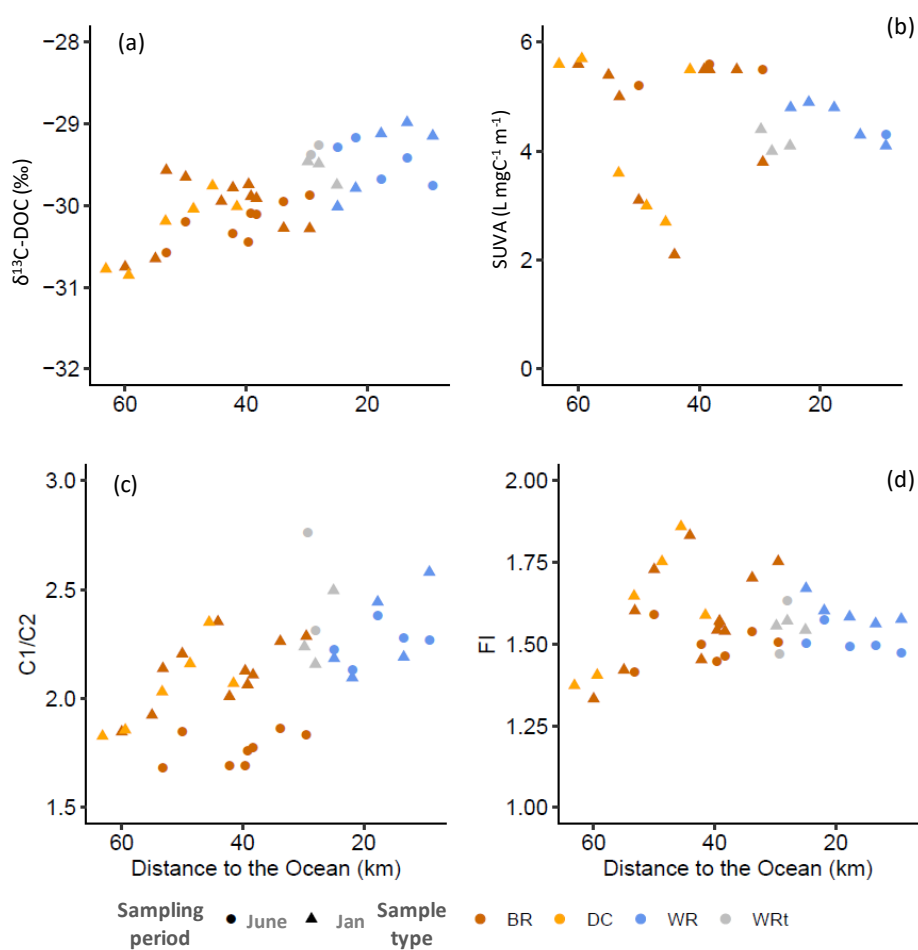
559

560

561



562
563
564
565
566
567



568

569 **Figure 3:** Evolution of DOM along the black river to the ocean continuum. (a) $\delta^{13}\text{C-DOC}$, (b) SUVA (Specific
570 UV Absorbance) index, (c) C1/C2, (d) FI (Fluorescence Index).

571

572

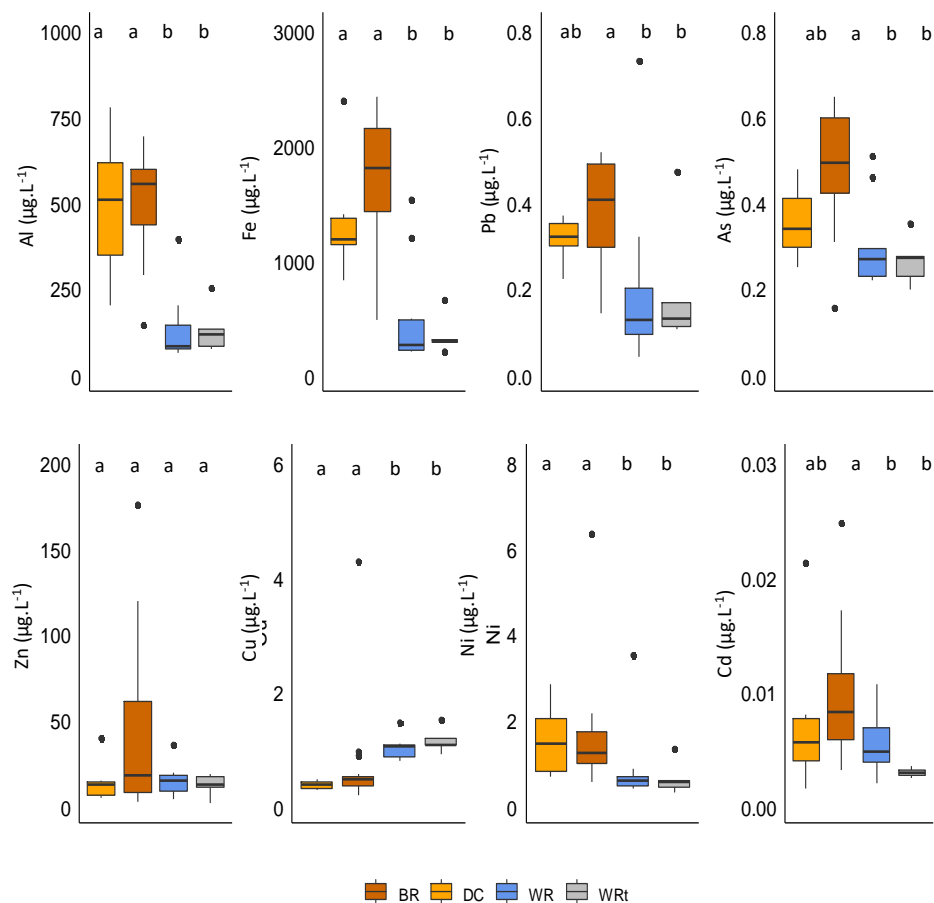


573

574

575

576



577

578 **Figure 4:** Ranges of selected TM concentration for different sampled water types. Letters represent significantly
 579 different groups (Kruskal Wallis and Dunn's post hoc multiple test ($p < 0.05$)).

580

581

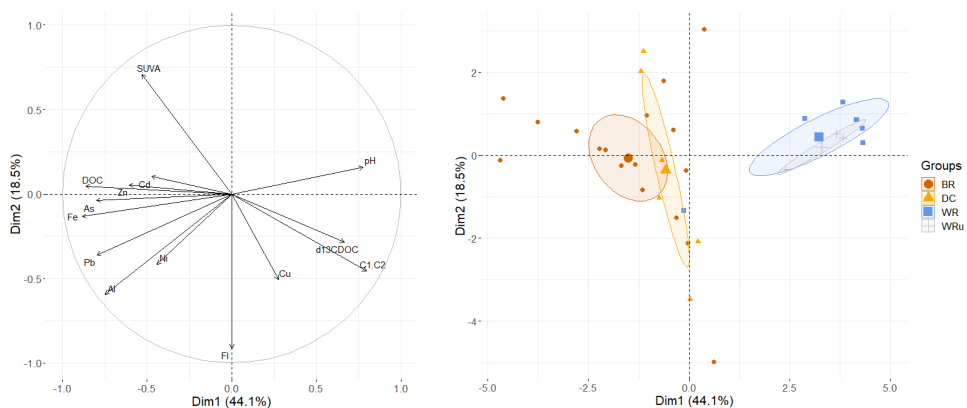
582

583

584



585
586
587
588
589



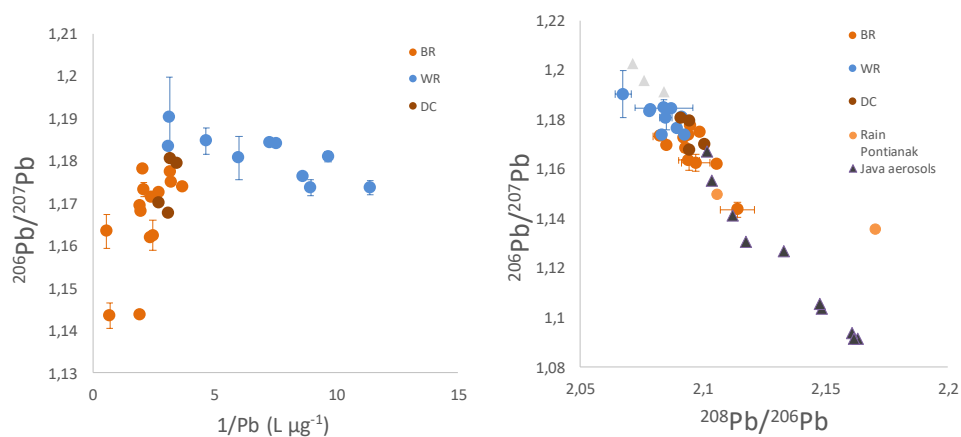
590
591

592 **Figure 5:** The first two factors of the PCA (63,1 % of variance) by variables (a) and by observation (b) for the
593 different sampled water types.

594
595
596
597
598
599
600
601
602
603
604
605
606
607



608
609
610
611
612
613
614
615



616
617
618
619
620
621
622

Figure 6: (a) Dependence of $^{206}\text{Pb}/^{207}\text{Pb}$ ratio on Pb concentrations for the different water samples. (b) Relationship between $^{206}\text{Pb}/^{207}\text{Pb}$ ratio and $^{208}\text{Pb}/^{206}\text{Pb}$ ratio.